Ca^{2+} Selectivity of a Chemically Modified OmpF with Reduced Pore Volume

Henk Miedema,* Maarten Vrouenraets,* Jenny Wierenga,* Dirk Gillespie,† Bob Eisenberg,† Wim Meijberg,* and Wolfgang Nonner‡

*Biomade Technology Foundation, Nijenborgh, Groningen, The Netherlands; †Department of Molecular Biophysics and Physiology, Rush University Medical Center, Chicago, Illinois; and ‡Department of Physiology and Biophysics, University of Miami Miller School of Medicine, Miami, Florida

ABSTRACT We studied an *E. coli* OmpF mutant (LECE) containing both an EEEE-like locus, typical of Ca^{2+} channels, and an accessible and reactive cysteine. After chemical modification with the cysteine-specific, negatively charged ($-1e$) reagents MTSES or glutathione, this LECE mutant was tested for Ca^{2+} versus alkali metal selectivity. Selectivity was measured by conductance and zero-current potential. Conductance measurements showed that glutathione-modified LECE had reduced conductance at Ca^{2+} mole fractions $<10^{-3}$. MTSES-modified LECE did not. Apparently, the LECE protein is (somehow) a better Ca^{2+} chelator after modification with the larger glutathione. Zero-current potential measurements revealed a Ca^{2+} versus monovalent cation selectivity that was highest in the presence of Li^+ and lowest in the presence of Cs^+. Our data clearly show that after the binding of Ca^{2+} the LECE pore (even with the bulky glutathione present) is spacious enough to allow monovalent cations to pass. Theoretical computations based on density functional theory combined with Poisson-Nernst-Planck theory and a reduced pore model suggest a functional separation of ionic pathways in the pore, one that is specific for small and highly charged ions, and one that accepts preferentially large ions, such as Cs^+.

INTRODUCTION

Electrostatic interactions play a key role in proteins (1,2) including ion channels (3,4), where they, directly and indirectly, produce ion selectivity (5–20). The signature sequence of voltage-activated Na^+ channels is made of a negatively charged aspartate (D) and glutamate (E), a positively charged lysine (K), and a neutral alanine (A), the so-called DEKA locus (21–23). The selectivity filter of Ca^{2+} channels is more negatively charged than the filter of the Na^+ channel, because it contains four acidic residues, either glutamates—the EEEE locus (24,25)—or two glutamates and two aspartates—the EEDD locus (26). Heinemann et al. (21) demonstrated that a single mutation in the DEKA locus (DEKA → DEEA) converts a Na^+ channel into a Ca^{2+} channel. Yamaoka et al. (27) showed that EEEE → DEKA mutations turn a Ca^{2+} channel into one that is selective for Na^+.

Apart from the net charge of the selectivity filter, another parameter that is crucial for ion selectivity is the pore diameter. Ion selectivity based on protein-ion interactions rather than just the relative mobilities in free solution becomes important when the channel radius and the Debye length (inside the channel) are of similar size (28–30). Pore dimensions play a key role in the charge space competition (CSC) model (7,31,32). The main role of structure in the model is to determine the space available in the selectivity filter. As a result, small changes in volume can have large effects on selectivity. After its successful application to the L-type Ca^{2+} channel (7), CSC theory proved to be a useful description of the selectivity of Na^+ channels (33,34), the channel of the ryanodine receptor (RyR) (35), and anion channels (36,37).

In a previous study, our lab engineered the *Escherichia coli* porin OmpF (15) to test whether the incorporation of negatively charged side chains can transform the essentially nonselective OmpF into a Ca^{2+}-selective channel, even though OmpF and natural Ca^{2+} channels are unrelated and could hardly be more dissimilar. The L-type Ca^{2+} channel structure uses α-helices to span the membrane, whereas the OmpF structure uses folded β-barrels. The 3D crystal structure of OmpF (38) shows a constriction zone about halfway through the channel that almost certainly forms the selectivity filter (39–41). Charged amino acid residues in this constriction zone determine the permeation properties of the channel (42,43). Our previous work on the LEAE mutant supports this view. LEAE contains an EEED locus and has a much higher cation over anion selectivity than wild-type (WT) OmpF (15). On the other hand, LEAE is hardly more selective for Ca^{2+} than Na^+, and so does not have one of the key properties of natural Ca^{2+} channels. The CSC model was consistent with our results—including the lack of Ca^{2+} versus Na^+ selectivity—given the large pore volume of the OmpF mutant we studied.

Here we continue to engineer OmpF mutants with improved Ca^{2+} over Na^+ selectivity. We started with an OmpF (cysteine) mutant LECE that has the same net charge and approximately the same volume as the previously characterized LEAE mutant (15). Recently, we have developed protocols to chemically modify OmpF with the cysteine-specific reagents MTSES and

Submitted April 13, 2006, and accepted for publication September 7, 2006.

Address reprint requests to W. Nonner, Dept. of Physiology and Biophysics, University of Miami, Miller School of Medicine, PO Box 016430, Miami, FL 33101-6430. E-mail: wnonner@chroma.med.miami.edu.

© 2006 by the Biophysical Society

0006-3495/06/12/4392/09 $2.00

doi: 10.1529/biophysj.106.087114

the tripeptide glutathione (GLT) (30). When these groups attach to a cysteine residue in the pore, they add negative charge, and reduce the volume available to ions in the pore. Glutathione is expected to have a particularly large effect on volume because it occupies approximately three times more space than MTSES (30).

Our two previous studies (15,30) compared and emphasized general differences between WT and (chemically modified) mutants. Here we focus on selectivity changes, specifically in Ca^{2+} versus monovalent cation selectivity produced by the chemical modification of the LECE mutant. If space in the channel for ions is as important as CSC theory suggests, the Ca^{2+} selectivity is expected to depend not only on the size of MTSES and GLT but also on the size of the monovalent cation species used. For that reason, the Ca^{2+} selectivity was studied and compared in Na^+, Li^+, Cs^+, and, to some extent, tetramethylammonium (TMA^+)-based solutions.

MATERIALS AND METHODS

Mutagenesis and chemical modification

The procedures for the site-directed mutagenesis, isolation, and purification of OmpF can be found in Miedema et al. (15). The chemical modification of refolded OmpF cysteine mutants with MTSES (Anatrace, Maumee, OH) and GLT (Sigma, Zwijndrecht, The Netherlands) is described in Vrouenraets et al. (30). Table 1 lists the characteristics of WT and the (modified) cysteine mutant LECE (K16L/R42E/R82C/R132E) used in this study. The numbers in Table 1 are based on a WT OmpF pore charge of $-1e$ (15), an LEAE mutant pore volume of 2 nm^3 (15), and the space occupied by individual amino acid residues and MTSES and GLT, all given in Vrouenraets et al. (30). Fig. 1 shows the constriction zone of WT and the LECE mutant as based on the crystal structure of WT (38).

Electrophysiology

The procedure of the planar lipid bilayer experiments, including pulse protocol and data analysis, follows (15). Briefly, 3 M KCl/2% agar salt bridges connected the *cis* compartment to the headstage of the Axopatch 200B amplifier (Axon Instruments, Foster City, CA) and the *trans* compartment to ground. The planar lipid bilayer was painted across a 250-μm-diameter aperture and was composed of phosphatidylethanolamine and phosphatidylcholine, in an 8:2 ratio (v/v) and dissolved in *n*-decane. OmpF stock solution,~0.2 μl of a 1- to 10-μg/ml, containing 1% (v/v) *n*-octyl-polyoxyethylene detergent (Alexis Biochemicals, San Diego, CA) was added to the *trans* side while stirring.

Conductances and zero-current or reversal potentials (E_{rev}) were determined from current traces in response to a voltage ramp that moved from -100 mV to 100 mV (in ~2 s). Data were low-pass filtered and digitized at 1 and 5 kHz, respectively. With the *trans* bath grounded, potential differences (V) are defined as $V = V_{cis} - V_{trans}$. A positive (outward) current (I) is defined as a flux of positive charge from *cis* to *trans*. Conductance is defined as the slope conductance (g) of the fully open trimer protein, as measured in the voltage range between -10 mV and 10 mV.

Phosphatidylethanolamine and phosphatidylcholine were purchased from Sigma (St. Louis, MO), and all other chemicals were from Aldrich (Milwaukee, WI). In NaCl solutions, the L-type Ca^{2+} channel is half-blocked at pH 7.5 (44). To prevent (putative) proton block of OmpF, all recording buffers contained 20 mM TAPS (pK = 8.4) and were adjusted to pH 9.0 with *N*-methyl-D-glucamine. Gradients are represented as *cis*//*trans*; for instance, a 0.1//1 M KCl gradient indicates 0.1 M KCl in the *cis* compartment and 1 M KCl in the *trans* compartment. Zero-current potentials have all been corrected for liquid junction potentials (LJP), which were either measured independently or calculated using Axon's pClamp9 software. Selectivity is expressed as the deviation of E_{rev} from the Nernst potentials of the relevant ion species.

TABLE 1 Characteristics of the (modified) LECE mutant used in this study

	Net Charge (e)	Volume (nm^3)
WT	-1	1.843
LECE*	-7	1.98
LECE-MTSES	-8	1.89
LECE-GLT	-8	1.67

*Amino acid substitutions in the LECE mutant: K16L, R42E, R82C, and R132E.

DFT/PNP simulations

Following previous simulations of WT and mutant porin (15), we consider a reduced model of LECE or LECE-GLT. The pore is represented as a central cylinder (radius 0.8 nm, length 1 nm) adjoined to 1 nm long atria that open with an angle of 45° into hemispherical baths of 10 nm radius. Fixed ion concentrations and electrical potentials are imposed at the external boundaries of the baths. Protein groups and GLT that extend into the pore lumen are represented as particles that are confined to the central cylinder but free to move anywhere within that confined volume. These include four carboxylate groups in LECE, or six carboxylate, one amino, and nine hydrocarbon groups in LECE-GLT. Ions were assigned crystal diameters (45), and the three kinds of protein groups were represented as spheres with diameters of 0.45, 0.3, and 0.374 nm, respectively. Water was modeled by hard spheres, 0.28 nm in diameter. The carboxylate and amino groups were assigned formal charges of $-1e$ and $+1e$. In addition, a charge of $-3e$, representing other charges that contribute to the overall negative net charge of porin, was smeared over the central cylinder volume (see Miedema et al. (15)). The dielectric coefficient was 80 throughout the domain.

A combination of density functional theory (DFT) and Poisson-Nernst-Planck theory (PNP) was used to predict experimental conductances for 10 mV applied potential and symmetrical baths containing 0.1 M mixtures of $CaCl_2$ and the chloride salt of one of the alkali metals—Li^+, Na^+, or Cs^+. Local excess chemical potentials were computed via DFT and included in the chemical potentials of the ions used in the PNP computations of flow. The DFT/PNP method used has been described in detail previously (9,46). The theory needs to be given estimates of diffusion coefficients. These external parameters (D_{Li}, D_{Na}, D_{Cs}, and D_{Ca}) were estimated from conductances measured in pure salt solutions (in 10^{-11} m^2/s): 0.5, 1.1, 1.55, and 0.1, respectively (in LECE), or 0.35, 0.8, 1.35, and 0.047, respectively (in LECE-GLT). The diffusion coefficients needed for LECE-GLT were smaller than those for LECE, as is expected from the reduction of free pore cross section by GLT. Calculations done for mixed solutions were based on the diffusion coefficients estimated for pure solutions. Lastly, a repulsive potential of 1 kT was assigned to water in the central cylinder of the pore to represent hydrophobic interactions important for the partitioning of Cs^+ ion (see Discussion). The value of this parameter is about one quarter the Gibbs energy of evaporation of bulk water at room temperature, and was chosen based on earlier work (36). No refinement was attempted.

RESULTS

Channel conductance in pure salts

Current-voltage (IV) relationships measured with (''symmetrical'') 0.1 M NaCl solutions on both sides are compared

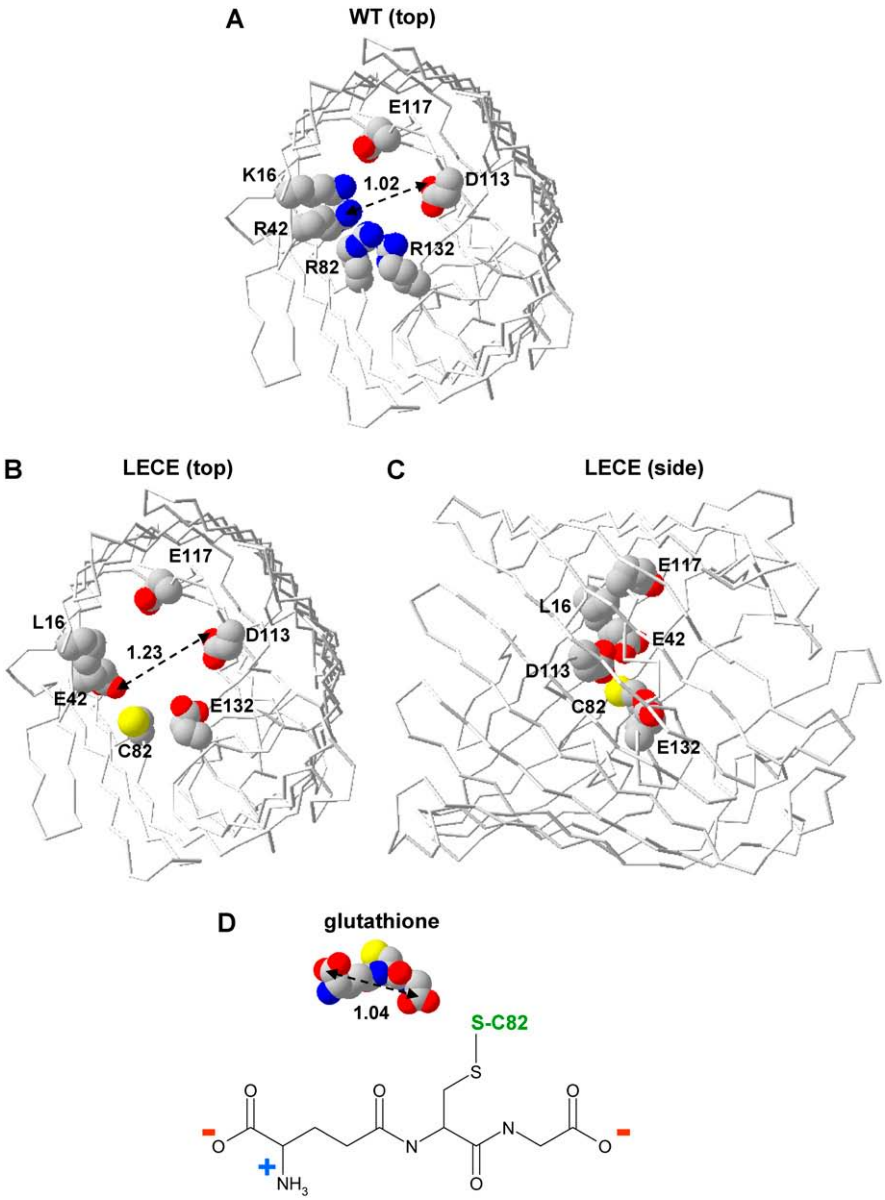

FIGURE 1 Images of WT and LECE mutant OmpF, and glutathione. (*A*) Top view of the constriction zone of a single monomer of WT. (*B*) Top view of the LECE mutant. (*C*) Side view of the LECE mutant. (*D*) Glutathione. Images, including the indicated measured distances (in nm), were prepared in SwissPdbViewer 3.7 (the shown spatial conformation of engineered side chains reflect choices made by this code).

in Fig. 2 *A* for WT OmpF and (modified) LECE mutant. LECE, LECE-MTSES, and LECE-GLT all conduct larger currents than WT with little change to the shape of the current-voltage relationship. LECE-GLT is less conductive than LECE or LECE-MTSES and has a slightly asymmetrical characteristic at potentials of large magnitude. Overall, the character of the *IV* relations is not substantially different from those of WT OmpF. Note that currents/conductances presented here are those of the trimer. The instantaneous current ''jumps'' as seen in some of the traces (e.g., that of LECE and LECE-GLT) reflect gating events (in this case of closure) of individual monomers. Fig. 2 *B* shows a summary of trimeric slope conductances (at 0 mV) determined in 0.1 M solutions of several pure salts (i.e., no Ca^{2+} added). In LiCl, NaCl, and CsCl, the conductance of the WT channel was always less than the conductances of (modified) LECE. WT conductance exceeded mutant conductance only when the relatively large molecule TMA^+ was the monovalent cation.

WT OmpF is permeable to both cations and anions. In pioneering work, Schirmer and Phale (47) showed (in simulations confirmed by Im and Roux (48,49)) that cations and anions permeate the OmpF pore using two different routes, marked by residues with negative or positive charges, respectively. Anions and cations see two different energy landscapes (along two different routes) for a given protein structure. In effect, the protein conformation (relevant for function) is different for anions and cations in OmpF. The variation of WT conductance (g) among LiCl, NaCl, and CsCl solutions ($g_{Li} < g_{Na} < g_{Cs}$) indicates that the cation route in WT OmpF is quite selective, preferring $Cs^+ > Na^+ > Li^+$.

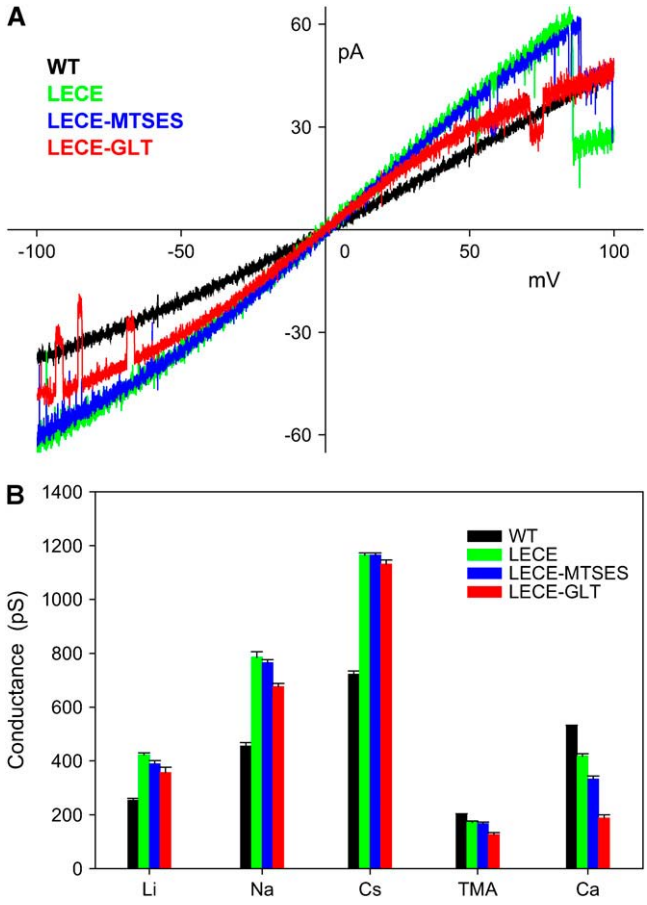

FIGURE 2 Overview of conduction in WT and LECE mutant channels: pure salts. (*A*) Current-voltage plots of WT, LECE, LECE-MTSES, and LECE-GLT in symmetrical 0.1 M NaCl solutions, pH 9, that are nominally Ca^{2+}-free. (*B*) Bar graph of slope conductances in Ca^{2+}-free 0.1 M solutions of alkali metal chlorides and TMA-Cl, and in 0.1 M $CaCl_2$, pH 9. Ionic crystal radius increases from Li^+ to TMA^+. Some standard deviations are too small to distinguish in the graph. Data are based on at least six independent measurements.

In the LECE mutant, four positively charged residues are replaced with two negative and two neutral residues (Fig. 1). In all experiments reported here, we try to ionize the introduced anionic groups by using test solutions of pH 9.0. The original positively charged residues form part of the ''anion route'' through the pore. This anion route in WT (the arginine cluster) has presumably been converted to a cation route in LECE. Indeed, measurements of zero-current potentials in salt gradients have shown that LECE and LEAE mutants are highly specific for cations over anions (15). We do not know to what extent the ''cation route'' of WT OmpF has been affected by the introduction of yet another negatively charged group, as in LECE-MTSES and LECE-GLT. What became evident, however, is that these modified LECE proteins show a cation selectivity that is even higher than that of the unmodified LECE mutant (30).

It is interesting to note that the cationic conductances of the modified LECE channels are always less than those of unmodified LECE (Fig. 2 *B*), presumably because the modified channels have less cross-sectional area and pore volume. One might expect that the relatively large groups introduced by the modifications into the pore would reduce the cross section available for conduction and thus reduce conductance. On the other hand, one might expect that the modified LECE channels would conduct cations better than LECE because their pores include an additional negative permanent charge. The additional permanent charge should increase the concentration of nearby counterions (cations) and increase cation conductance, if the mobility of individual cations is not changed. In fact, the net effect always is a reduced conductance, with the amount of reduction dependent on the type of salt. Cs^+ is conducted best in all channels; Li^+ is conducted least well. These experiments with monovalent cations reveal that the (modified) LECE mutant conducts large alkali metal ions better than small ones. The effect of engineering is a mild increase in selectivity among the alkali metal cations compared to WT OmpF. This is also consistent with the pattern seen in L-type Ca^{2+} channels, whose conduction pattern we seek to approximate by engineering OmpF.

Interestingly, even in the case of the rather large cation TMA^+, the reduction of the pore cross section by GLT is not enough to prevent substantial permeation (Fig. 2 *B*). The fact that WT and mutant channels conduct TMA-Cl similarly likely implies a partial compensation of several effects, given that WT, but not the mutant, can conduct Cl^- because WT is essentially nonselective.

Last, Fig. 2 *B* also includes conductances measured in symmetrical pure 0.1 M $CaCl_2$ solutions. In the WT channel, the conductance for $CaCl_2$ is larger than that for any alkali metal salt, with the exception of CsCl. In (modified) LECE, the conductance for $CaCl_2$ is always smaller than, or the same as, the conductance for alkali metal salts, with LECE-GLT giving the smallest conductance. The relatively large $CaCl_2$ conductance in the WT channel includes a substantial anionic component, which by itself may account for the observation that the conductance in 0.1 M $CaCl_2$ is larger than in a 0.1 M alkali metal salt. In the (modified) LECE mutant, the conductance in $CaCl_2$ reflects the fact that only Ca^{2+} moves through the channel. Here, the Ca^{2+} conductance of the modified LECE porins is smaller than that of unmodified LECE. Indeed, in LECE-GLT, the Ca^{2+} conductance is substantially smaller than the conductance in the presence of any of the alkali metal ions. The behavior of the mutants is a deviation from the behavior of WT and is a change toward the behavior seen in L-type Ca^{2+} channels, where (for example) Na^+ conductance is about an order of magnitude larger than Ca^{2+} conductance (50).

Channel conductance in mixed solutions

In L-type Ca^{2+} channels, the most striking sign of Ca^{2+} selectivity (over alkali metal cations) is a large reduction (''blockade'') of monovalent cation current by micromolar

amounts of Ca^{2+} added to the extracellular solution (51,52). These channels are thought to accumulate Ca^{2+} in the pore in molar concentrations from micromolar Ca^{2+} in the bath, thereby favoring the conduction of Ca^{2+} over alkali metal ions like Na^+. Fig. 3 *A* plots slope conductances of WT OmpF measured in symmetrical solutions of LiCl, NaCl, or CsCl including a varied mole fraction of $CaCl_2$. The leftmost data points are measurements in nominally pure 0.1 M monovalent salt solutions. No Ca^{2+} was added to these solutions but for graphing the data we assumed a Ca^{2+} contamination of 0.1 μM (calcium mole fraction (CMF) = 10^{-6}). Adding 50 μM EDTA to the nominally pure 0.1 M LiCl, NaCl, and CsCl solutions (at pH 9) did not significantly change the conductance of the LECE-GLT mutant (results not shown). Because adding 1 μM $CaCl_2$ to nominally pure alkali metal solutions (CMF = 10^{-5}) had a significant effect on the LECE-GLT conductance (Fig. 3 *D*), we conclude that the Ca^{2+} contamination in the 0.1 M alkali metal salt solutions was <1 μM. The rightmost data points in Fig. 3 *A* refer to solutions with nominally pure 0.1 M $CaCl_2$ (CMF = 1). Fig. 3, *B–D*, shows analogous results for unmodified LECE (*B*), LECE-MTSES (*C*), and LECE-GLT (*D*). Note that the cases of CMF = 10^{-6} and CMF = 1 have already been discussed in the previous section.

The conductances of the WT channel are rather insensitive to $CaCl_2$ mole fraction and the direction of the observed small changes depends on the alkali metal species. By contrast, the conductances of (modified) LECE are substantially reduced with increasing $CaCl_2$ mole fraction. In some cases, conductance passes through a minimum before CMF = 1 is reached, thus showing anomalous mole-fraction behavior. In the L-type Ca^{2+} channel, 1 μM Ca^{2+} (CMF = 10^{-5}) suffices to block half of the Na^+ current (51,52). For comparison, a substantial reduction of the monovalent cation current through our engineered OmpF channels requires 10^2- to 10^3-times-larger mole fractions of Ca^{2+}.

Closer inspection of Fig. 3 *D* reveals that in LECE-GLT the conductance drops in a stepwise manner as the mole fraction of Ca^{2+} is increased. A partial reduction at CMF $<$ 10^{-4} is followed by further reduction at CMF $\geq$ 10^{-3}, regardless of the species of alkali metal ion competing with Ca^{2+}. The drop in conductance at CMF $<$ 10^{-4} reveals that Ca^{2+} interacts with this modified channel at low micromolar concentrations. On the other hand, the interaction controls conductance only to a partial extent, as if not all routes for alkali metal ion conduction were blocked by the Ca^{2+} accumulated in some part of the pore. This kind of sensitivity to Ca^{2+} is not observed in LECE-MTSES (which has the same net charge as LECE-GLT). The curves in Fig. 3, *B* and *D*, have been computed using a combination of DFT and PNP theory as described in Methods. Their relationship to the experimental points will be discussed later.

The current-voltage relations of the LECE-GLT mutant shown in Fig. 4 were measured using solutions of 0.1 M NaCl on both sides, with (trace *b*, *gray*) and without (trace *a*, *black*) 2 mM $CaCl_2$ added to the *trans* solution. Unlike the current-voltage relation seen in the Ca^{2+}-free experiment, the current-voltage relation shows substantial rectification when Ca^{2+} is present on the *trans* side. Current is reduced in both directions, but more so in the *trans*-to-*cis* direction. Apparently, Na^+ flow is reduced to the extent that Ca^{2+} is driven into the pore. A small amount of Ca^{2+} added on one side thus has a substantial effect on overall conductance. The currents shown correspond to the fully open OmpF trimer as is illustrated by a second sweep of the 2 mM Ca^{2+} trace in Fig. 4, in which the closure of all three monomers occurred at negative potentials (trace *c*, *dark gray*). Thus, the reduction of current in the presence of Ca^{2+} compared to the current in

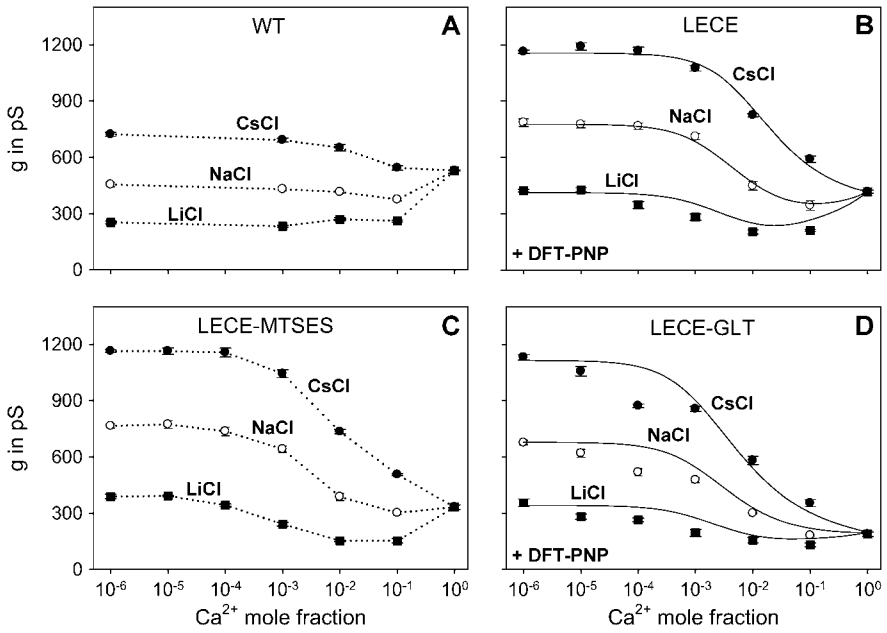

FIGURE 3 Effect of $CaCl_2$ mole fraction on slope conductance. Data from WT (*A*) and (modified) LECE mutant (*B–D*) in LiCl, NaCl, and CsCl solutions, pH 9, containing a varied mole fraction of $CaCl_2$ (CMF). Data from nominally pure 0.1 M alkali metal salts are plotted at CMF 10^{-6} (see text). Each data point is based on at least six independent measurements. Some standard deviations are smaller than the symbol size. Dotted lines in *A* and *C* just connect the experimental data points, whereas the solid lines in *B* and *D* represent DFT-PNP calculations (see text).

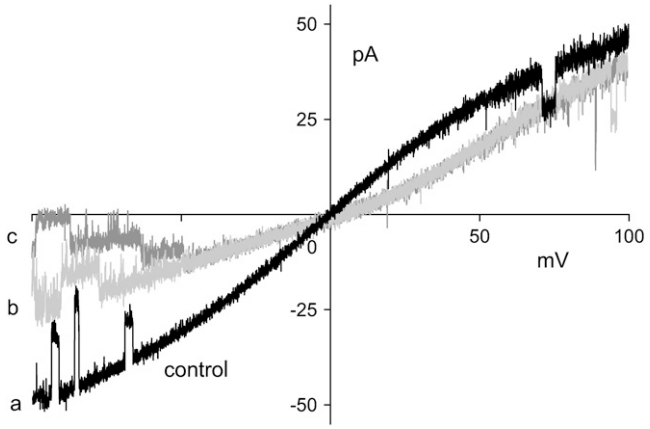

FIGURE 4 Current rectification of LECE-GLT as induced by unilateral addition of $CaCl_2$. Symmetrical 0.1 M NaCl, pH 9, with 2 mM $CaCl_2$ present on the *trans* side only. The slightly positive E_{rev} of ~4 mV in the presence of Ca^{2+} (traces *b* and *c*) indicates that Ca^{2+} is permeant. The control trace *a* (*black*) was recorded in the absence of Ca^{2+}; trace *c* (*dark gray*) exemplifies the gating of individual monomers. Voltages applied in the presence of Ca^{2+} have been corrected for an LJP of −0.4 mV.

pure NaCl solutions is not a gating effect, i.e., it is not produced by the closure of monomers.

Zero-current potential

The small positive zero-current potential of the 2 mM Ca^{2+} traces of Fig. 4 indicates that Ca^{2+} current has a role in determining the value of the zero-current potential. We further investigated the Ca^{2+} selectivity by measuring zero-current potentials (53) in symmetrical 0.1 M concentrations of alkali metal chlorides, with either 2 mM or 0.1 M $CaCl_2$ present in the *trans* solution only. Fig. 5 *A* summarizes the zero-current potentials of (modified) LECE protein, using NaCl as the alkali metal salt. The results are not significantly different among these three channels. The zero-current potentials are closer to the equilibrium (Nernst) potential for Na^+ (i.e., closer to zero) than to the equilibrium potential for Ca^{2+}. The equilibrium potential for Ca^{2+} is very large and positive, limited only by the contamination level of Ca^{2+} in the *cis* solution. The difference in zero-current potentials measured in the 0.1 M and 2 mM Ca^{2+} concentrations is of order 20 mV, which is clearly less than the difference in equilibrium potentials for Ca^{2+} expected for these concentrations. (The expected difference is ~45 mV (see Fig. 5 *A*).) Thus, Ca^{2+} contributes substantially to the zero-current potential, but it does not dominate the potential. The contribution of Na^+ to E_{rev} marks an essential difference between our engineered OmpF mutants and natural, highly selective L-type Ca^{2+} channels (50).

A further difference between the engineered OmpF channels and L-type Ca^{2+} channels is observed in ''high'' Ca^{2+} solutions with a background of either Li^+, Na^+, or Cs^+ (Fig. 5 *B*). The zero-current potential increases in magnitude in the order $Cs^+ < Na^+ < Li^+$. L-type Ca^{2+} channels have

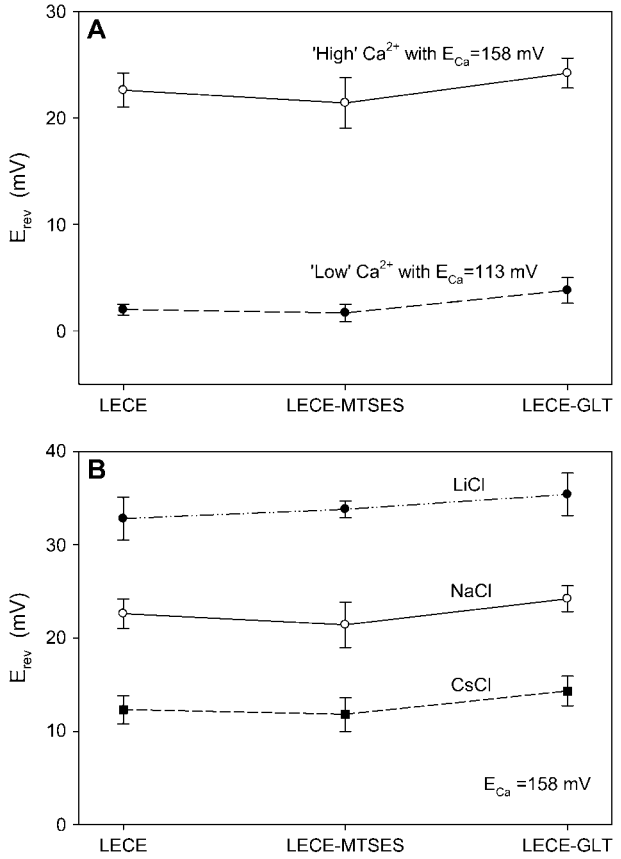

FIGURE 5 Assessment of Ca^{2+} permeability through zero-current potentials. (*A*) Symmetrical 0.1 M NaCl solution with 2 mM or 0.1 M $CaCl_2$ added on the *trans* side, pH 9. The indicated Ca^{2+} equilibrium potentials (E_{Ca}) are estimated assuming a Ca^{2+} activity of 0.1 μM in the 0.1 M NaCl solution. Computed Na^+ and Cl^- equilibrium potentials are −4 mV and −26 mV (with 0.1 M $CaCl_2$), and 0 mV and −1 mV (with 2 mM $CaCl_2$). Values of E_{rev} have been corrected for an LJP of −0.4 mV and −9 mV in ''low'' and ''high'' Ca^{2+} solutions, respectively. (*B*) E_{rev} in high Ca^{2+} solutions with a 0.1 M symmetrical background of either Li^+, Na^+, or Cs^+ chloride. These E_{rev} values have been corrected for an LJP of −9 mV. Each data point is based on at least six independent measurements.

the opposite order. By this criterion, the (modified) LECE proteins are more permeable to Cs^+ than to Li^+ when Ca^{2+} is present; L-type Ca^{2+} channels are more permeable to Li^+ than Cs^+. LECE and LECE-GLT show a higher selectivity for Cs^+ than for Li^+ also under bi-ionic conditions in Ca^{2+}-free solutions (Table 2).

DISCUSSION

The LECE-GLT mutant of OmpF represents progress in our attempt to engineer a channel comparable in selectivity to a natural L-type Ca^{2+} channel in which alkali metal ion currents are partially blocked by micromolar amounts of Ca^{2+}. The blockage effect is less profound in the other chemically modified mutant, LECE-MTSES. The two modifications differ in several structural aspects including the kind of introduced

TABLE 2 Zero-current potentials (E_{rev}) of LECE and LECE-GLT under bi-ionic conditions, pH 9, with E_K and E_{Cs} at $-\infty$ mV

Cis//*trans trans* grounded	LECE E_{rev} (mV)	LECE-GLT E_{rev} (mV)
0.1 M KCl // 0.1 M NaCl	−9.3 ± 0.9	−9.5 ± 1.2
0.1 M CsCl // 0.1 M LiCl	−22.0 ± 1.0	−22.1 ± 1.9

E_{rev} values have been corrected for an LJP of −4.3 mV (in KCl//NaCl) and −7.3 mV (in CsCl//LiCl). Data are based on at least six independent measurements.

anionic group, the length of the introduced chain, and the volume displaced by the group and chain. Does the longer chain of GLT allow its anionic group to chelate Ca^{2+} in a way not possible for the MTSES compound? How severe is the pore constriction created by the volume of GLT? These questions will need to be addressed by structural analysis of these proteins.

Although LECE-GLT does not yet qualify as a classic Ca^{2+} channel, it does have many of the properties of the RyR Ca^{2+} channel that releases Ca^{2+} from the sarcoplasmic reticulum. Like LECE-GLT, RyR is a high-conductance cation channel with monovalent conductances of ~200 pS for LiCl, ~500–550 pS for NaCl and CsCl, and ~800 pS for KCl in 250 mM symmetric solutions (35). (In comparison, the monovalent conductances of the L-type Ca^{2+} channel are 5–10 times smaller (54).) Fig. 2 *B* shows that LECE-GLT has monovalent conductances in 100 mM solutions almost twice as large as RyR in 250 mM solutions. The monovalent versus Ca^{2+} selectivity of LECE-GLT and RyR are also similar. For example, in RYR the addition of millimolar $CaCl_2$ to 250 mM NaCl, KCl, and CsCl measurably reduces the monovalent current (35). This is similar to the second-stage reduction of current in LECE-GLT (Fig. 3). In both RyR and LECE-GLT, unilateral addition of millimolar $CaCl_2$ to a symmetrical background of alkali metal chloride yields zero-current potentials much smaller than expected from a high specificity for Ca^{2+}. On the other hand, in LECE-GLT the magnitude of these reversal potentials depends more strongly on the species of the alkali metal (Fig. 5 *B*) than in RyR (35).

Despite micromolar Ca^{2+} binding having been achieved in the OmpF pore (in LECE-GLT, Ca^{2+} starts to reduce current at CMFs as low as 10^{-5}, i.e., at 1 μM Ca^{2+} (see Fig. 3 *D*)), a major problem remains: the binding of Ca^{2+} in the engineered pore does not shut down alkali metal ion flux as much as it shuts down a natural L-type Ca^{2+} channel. Our mutations and modifications to OmpF all involve residues that carry positively charged side chains in WT OmpF and likely are part of the pathway for anions in the WT channel. The WT channel, however, also carries a substantial cation current, perhaps through a different pathway in this wide pore. It is therefore possible that we have engineered a channel in which a pathway, in WT channels present as the anion route, is replaced by a pathway that has high affinity for Ca^{2+} and small monovalent cations. The transformation of the WT anion route into one that conducts cations only is supported by zero-current-potential measurements on these chemically modified mutants that showed E_{rev}s essentially equal to E_{cation} (30). In addition, a bypass pathway, in WT channels present as the cation route, appears to be more or less preserved in our mutants and conducts all cations found in the bulk solutions used. This interpretation, based on our low-resolution DFT/PNP calculations, is reminiscent of the two parallel pathways suggested by Brownian dynamics and molecular dynamics simulations on WT OmpF (47–49). In that case, our measurements reflect the flow of current in two parallel pathways. The selective conductance of the calcium pathway could be obscured by the parallel conductance of the bypass. To be consistent with our results, such a bypass would have to conduct alkali metals with the preference $Cs^+ > Na^+ > Li^+$. The cation selectivity of WT OmpF is $Cs^+ > Na^+ > Li^+$, suggesting that this WT bypass for cations is (more or less) still intact in LECE-GLT, in parallel with the (engineered) highly Ca^{2+}-selective pathway.

The possibility of different permeation pathways in a pore of unknown crystallographic structure precludes a detailed analysis of the physics that dominates conductance in LECE-GLT. We can, however, use a theory of lower resolution to connect conjectures about structure with the conductances that we observe. The approach that we use is a combination of DFT and PNP theory. We have applied DFT/PNP theory in an earlier study of porin mutants (15); a study on ryanodine receptor channels has related a wide range of conduction data using a DFT/PNP description and a pore model reduced to essential charged groups (35). Here, we ask to what extent a ''null hypothesis'' regarding the structure of the LECE and LECE-GLT pores can produce the observed mole-fraction behaviors. Specifically, we will assume that the functional groups of LECE or LECE-GLT are confined to the pore but are not sterically restricted in any a priori way to form discrete paths for conduction. The curves shown in Fig. 3, *B* and *D*, have been computed from such models of LECE and LECE-GLT (for details, see Methods).

A comparison between the experimental and theoretical conductances in Fig. 3, *B* and *D*, shows that the theory predicts conductances measured in the presence of millimolar Ca^{2+} quite well. The theory, however, predicts too-large (monovalent-ion) conductances compared with those observed in LECE-GLT in the presence of smaller mole fractions of Ca^{2+}. This difference might arise because in the model the anionic groups of the channels are too dilute to capture Ca^{2+} ion in a chelate because the volume of our channel is too large. If this is true, the observed behavior of the conductance at low Ca^{2+} mole fractions could reflect a ''Ca^{2+} pathway'' that is preformed by sterical constraints that align the anionic groups so they create a separate pathway.

The model captures the distinct mole fraction behavior observed when Ca^{2+} competes with different alkali metal cations. Anomalous mole fraction behavior, involving a minimum of conductance, is predicted for Li^+; not predicted for

Cs^+; and predicted to different extents for Na^+ in LECE and LECE-GLT, respectively. To predict the conductance effects with Cs^+ correctly, the model includes a parameter that describes a hydrophobic component of the milieu of the pore. This parameter is an energetic penalty (1 kT) assigned to water molecules dwelling in the narrow region of the pore. The energetic penalty slightly reduces the packing density of water in that region, and thereby modifies the excluded-volume component of the local excess chemical potentials of particles. Its selectivity effect is to facilitate the partitioning of large particles (such as Cs^+) from the bulk solution into the pore (36,37). The energetic penalty for water is much less important for the partitioning of small particles such as Li^+, Na^+, or Ca^{2+}. In computations that did not include this hydrophobicity component in the model, robust anomalous mole fraction behavior was predicted also for mixtures of Ca^{2+} with Cs^+, contrary to the experimental result. Our modeling therefore suggests that the ability of Cs^+ to compete with millimolar Ca^{2+} in such a way as our experiments indicate (no anomalous mole fraction effects) requires an additional structural feature of the pore in the form of hydrophobicity. This supports the idea that parts of the walls of both the LECE and LECE-GLT pores provide a hydrophobic lining that—via its effect on the water—allows the large cation, Cs^+, to dwell in the pore even when the baths contain millimolar Ca^{2+} concentrations.

In conclusion, our theoretical analysis suggests that conduction in the pores of LECE and notably LECE-GLT involves structural organizations beyond those included in our null hypothesis. Two ionic paths, one characterized by high anionic charge density, the other having a partially hydrophobic nature, might coexist in these engineered pores.

The authors are most grateful for the valuable input of the reviewers, in particular for the suggestion to interpret our experimental findings using a theoretical analysis.

This research is supported by NanoNed, a nanotechnology program of the Dutch Ministry of Economic Affairs. The work was supported in part by National Institutes of Health grant GM076013-01 to B.E.

REFERENCES

1. Warshel, A., and S. T. Russell. 1984. Calculations of electrostatic interactions in biological systems and in solutions. *Q. Rev. Biophys.* 17:283–422.
2. Honig, B., and A. Nicholls. 1995. Classic electrostatics in biology and chemistry. *Science.* 268:1144–1149.
3. Barcilon, V., D. P. Chen, and R. S. Eisenberg. 1992. Ion flow through narrow membrane channels: Part II. *SIAM J. Appl. Math.* 52:1405–1425.
4. Eisenberg, R. S. 1996. Computing the field in proteins and channels. *J. Membr. Biol.* 150:1–15.
5. Hollerbach, U., D. Chen, W. Nonner, and B. Eisenberg. 1999. Three-dimensional Poisson-Nernst-Planck theory of open channels. *Biophys. J.* 76:A205. (Abstr.)
6. Kurnikova, M. G., R. D. Coalson, P. Graf, and A. Nitzan. 1999. A lattice relaxation algorithm for 3D Poisson-Nernst-Planck theory with application to ion transport through the gramicidin A channel. *Biophys. J.* 76:642–656.
7. Nonner, W., L. Catacuzzeno, and B. Eisenberg. 2000. Binding and selectivity in L-type Ca^{2+} channels: a mean spherical approximation. *Biophys. J.* 79:1976–1992.
8. Schuss, Z., B. Nadler, and R.S. Eisenberg. 2001. Derivation of PNP equations in bath and channel from a molecular model. *Phys. Rev. E.* 64:036116.
9. Gillespie, D., W. Nonner, and R. S. Eisenberg. 2002. Coupling Poisson-Nernst-Planck and density functional theory to calculate ion flux. *J. Phys. Condens. Mat.* 14:12129–12145.
10. Eisenberg, B. 2003. Proteins, channels and crowded ions. *Biophys. Chem.* 100:507–517.
11. Mamonov, A. B., R. D. Coalson, A. Nitzan, and M. G. Kurnikova. 2003. The role of the dielectric barrier in narrow biological channels: a novel composite approach to modeling single-channel currents. *Biophys. J.* 84:3646–3661.
12. Nadler, B., U. Hollerbach, and R.S. Eisenberg. 2003. Dielectric boundary force and its crucial role in gramicidin. *Phys. Rev. E.*, 68:021905.
13. Nimigean, C. M., J. S. Chappie, and C. Miller. 2003. Electrostatic tuning of ion conductance in potassium channels. *Biochemistry.* 42: 9263–9268.
14. Aboud, S., D. Marreiro, M. Saraniti, and R. Eisenberg. 2004. A Poisson P3M force field scheme for particle-based simulations of ionic liquids. *J. Comp. Electr.* 3:117–133.
15. Miedema, H., A. Meter-Arkema, J. Wierenga, J. Tang, B. Eisenberg, W. Nonner, H. Hektor, D. Gillespie, and W. Wim Meijberg. 2004. Permeation properties of an engineered bacterial OmpF porin containing the EEEE-locus of Ca^{2+} channels. *Biophys. J.* 87:3137–3147.
16. Nadler, B., Z. Schuss, U. Hollerbach, and R.S. Eisenberg. 2004. Saturation of conductance in single ion channels: The blocking effect of the near reaction field. *Phys. Rev. E.*, 70:051912.
17. Noskov, S. Y., S. Bernèche, and B. Roux. 2004. Control of ion selectivity in potassium channels by electrostatic and dynamic properties of carbonyl ligands. *Nature.* 431:830–834.
18. van der Straaten, T. A., G. Kathawala, R. S. Eisenberg, and U. Ravaioli. 2004. BioMOCA: a Boltzmann transport Monte Carlo model for ion channel simulation. *Mol. Simul.* 31:151–171.
19. Corry, B., T. Vora, and S.-H. Chung. 2005. Electrostatic basis of valence selectivity in cationic channels. *Biochim. Biophys. Acta.* 1711: 72–86.
20. Merzlyak, P. G., M.-F. P. Capistrano, A. Valeva, J. J. Kasianowicz, and O. V. Krasilnikov. 2005. Conductance and ion selectivity of a mesoscopic protein nanopore probed with cysteine scanning mutagenesis. *Biophys. J.* 89:3059–3070.
21. Heinemann, S. H., H. Terlau, W. Stühmer, K. Imoto, and S. Numa. 1992. Calcium channel characteristics conferred on the sodium channel by single mutations. *Nature.* 356:441–443.
22. Favre, I., E. Moczydlowski, and L. Schild. 1996. On the structural basis for ionic selectivity among Na^+, K^+, and Ca^{2+} in the voltage-gated sodium channel. *Biophys. J.* 71:3110–3125.
23. Sun, Y.-M., I. Favre, L. Schild, and E. Moczydlowski. 1997. On the structural basis for size-selective permeation of organic cations through the voltage-gated sodium channel. *J. Gen. Physiol.* 110:693–715.
24. Yang, J., P. T. Ellinor, W. A. Sather, J. I. F. Zhang, and R. W. Tsien. 1993. Molecular determinants of Ca^{2+} selectivity and ion permeation in L-type Ca^{2+} channels. *Nature.* 366:158–161.
25. Cibulsky, S. M., and W. A. Sather. 2000. The EEEE locus is the sole high-affinity Ca^{2+} binding structure in the pore of a voltage-gated Ca^{2+} channel. Block by Ca^{2+} entering from the intracellular pore entrance. *J. Gen. Phys.* 116:349–362.
26. Talavera, K., M. Staes, A. Janssens, N. Klugbauer, G. Droogmans, F. Hofman, and B. Nilius. 2001. Aspartate residues of the Glu-Glu-Asp-Asp (EEDD) pore locus control selectivity and permeation of the T-type Ca^{2+} channel α_{1G}. *J. Biol. Chem.* 276:45628–45635.
27. Yamaoka, K., E. Kinoshita, and I. Seyama. 2003. Altering ion selectivity of the L-type Ca^{2+} channel cloned from frog cardiac myocytes. *Biophys. J.*. 84:402a. (Abstr.).

28. Kienker, P. K., and J. D. Lear. 1995. Charge selectivity of the designed uncharged peptide ion channel Ac-$(LSSLLSL)_3$-$CONH_2$. *Biophys. J.* 68:1347–1358.

29. Gu, L.-Q., M. D. Serra, J. B. Vincent, G. Vigh, S. Cheley, O. Braha, and H. Bayley. 2000. Reversal of charge selectivity in transmembrane protein pores by using noncovalent molecular adapters. *Proc. Natl. Acad. Sci. USA.* 97:3959–3964.

30. Vrouenraets, M., J. Wierenga, W. Meijberg, and H. Miedema. 2006. Chemical modification of the bacterial porin OmpF: gain of selectivity by volume reduction. *Biophys. J.* 90:1202–1211.

31. Nonner, W., and B. Eisenberg. 1998. Ion permeation and glutamate residues linked by Poisson-Nernst-Planck theory in L-type calcium channels. *Biophys. J.* 75:1287–1305.

32. McCleskey, E. W. 2000. Ion channel selectivity using an electric stew. *Biophys. J.* 79:1691–1692.

33. Boda, D., D. D. Busath, B. Eisenberg, D. Henderson, and W. Nonner. 2002. Monte Carlo simulations of ion selectivity in a biological Na channel: charge-space competition. *Phys. Chem. Chem. Phys.* 4:5154–5160.

34. Gillespie, D., W. Nonner, and R. S. Eisenberg. 2002. Physical model of selectivity and flux in Na channels. *Biophys. J.* 84:67a. (Abstr.).

35. Gillespie, D., L. Xu, Y. Wang, and G. Meissner. 2005. (De)constructing the ryanodine receptor: modeling ion permeation and selectivity of the calcium release channel. *J. Phys. Chem. B.* 109:15598–15610.

36. Gillespie, D., W. Nonner, D. Henderson, and R. S. Eisenberg. 2002. A physical mechanism for large-ion selectivity of ion channels. *Phys. Chem. Chem. Phys.* 4:4763–4769.

37. Roth, R., and D. Gillespie. 2005. Physics of size selectivity. *Phys. Rev. Lett.* 95:247801.

38. Cowan, S. W., T. Schirmer, G. Rummel, M. Steiert, R. Ghosh, R. A. Pauptit, J. N. Jansonius, and J. P. Rosenbusch. 1992. Crystal structures explain functional properties of two *E. Coli* porins. *Nature.* 358:727–733.

39. Schirmer, T. 1998. General and specific porins from bacterial outer membranes. *J. Struct. Biol.* 121:101–109.

40. Schulz, G. E. 2002. The structure of bacterial outer membrane proteins. *Biochem. Biophys. Acta.* 1565:308–317.

41. Delcour, A. H. 2003. Solute uptake through general porins. *Front. Biosci.* 8:1055–1071.

42. Saint, N., K.-L. Lou, C. Widmer, M. Luckey, T. Schirmer, and J. P. Rosenbusch. 1996. Structural and functional characterization of OmpF porin mutants selected for larger pore size. *J. Biol. Chem.* 271:20676–20680.

43. Phale, P. S., A. Philippsen, C. Widmer, V. P. Pahe, J. P. Rosenbusch, and T. Schirmer. 2001. Role of charged residues at the OmpF porin channel constriction probed by mutagenesis and simulation. *Biochemistry.* 40:6319–6325.

44. Pietrobon, D., B. Prod'hom, and P. Hess. 1989. Interactions of protons with single open L-type calcium channels. *J. Gen. Phys.* 94:1–21.

45. Nonner, W., D. Gillespie, D. Henderson, and B. Eisenberg. 2001. Ion accumulation in a biological calcium channel: Effects of solvent and confining pressure. *J. Phys. Chem. B.* 105:6427–6436.

46. Gillespie, D., W. Nonner, and R. S. Eisenberg. 2003. Density functional theory of charged hard-sphere fluids. *Phys. Rev. E.* 68:031503.

47. Schirmer, T., and P. S. Phale. 1999. Brownian dynamics simulation of ion flow through porin channels. *J. Mol. Biol.* 294:1159–1167.

48. Im, W., and B. Roux. 2002. Ions and counterions in a biological channel: a molecular dynamics simulation of OmpF porin from *Escherichia coli* in an explicit membrane with 1 M KCl aqueous salt solution. *J. Mol. Biol.* 319:1177–1197.

49. Im, W., and B. Roux. 2002. Ion permeation and selectivity of OmpF porin: a theoretical study based on molecular dynamics, Brownian dynamics, and continuum electrodiffusion theory. *J. Mol. Biol.* 322:851–869.

50. Hess, P., J. B. Lansman, and R. W. Tsien. 1986. Calcium channel selectivity for divalent and monovalent cations. Voltage and concentration dependence of single channel current in ventricular heart cells. *J. Gen. Physiol.* 88:293–319.

51. Almers, W., and E. W. McCleskey. 1984. Non-selective conductance in calcium channels of frog muscle: calcium selectivity in a single-file pore. *J. Physiol.* 353:585–608.

52. Hess, P., and R. W. Tsien. 1984. Mechanism of ion permeation through calcium channels. *Nature.* 309:453–456.

53. Gillespie, D., and R. S. Eisenberg. 2002. Physical description of experimental selectivity measurements in ion channels. *Eur. Biophys. J.* 31: 454–466.

54. Hess, P., J. B. Lansman, and R. W. Tsien. 1986. Blockade of current through single calcium channels by Cd^{2+}, Mg^{2+}, and Cd^{2+}. Voltage and concentration dependence of calcium entry into the pore. *J. Gen. Physiol.* 88:321–347.